Electronic Supplementary Material (ESI) for RSC Advances

[Supporting Information]

Phenanthroline diimide as an organic electron-injecting material for organic light-emitting devices

Hyena Lee,[a‡] Gwijeong Cho,[a,b,c‡] Sungho Woo,[a,c] Sungho Nam,[a] Jaehoon Jeong,[a,c] Hwajeong Kim,[a,d]* and Youngkyoo Kim*[a]

[a] Organic Nanoelectronics Laboratory, Department of Chemical Engineering, Kyungpook National University, Daegu 702-701, Republic of Korea.

[b] OLED Device Development Team, LG Display Co., Ltd, Paju-si, Gyeonggi-do 413-811, Republic of Korea

[c] Green Energy Research Division, DGIST, Daegu 711-873, Republic of Korea

[d] Priority Research Center, Research Institute of Advanced Energy Technology, Kyungpook National University, Daegu 702-701, Republic of Korea.

[‡]Hyena Lee and Gwijeong Cho contributed equally to this work.

E-mail: (ykimm@knu.ac.kr, khj217@knu.ac.kr)

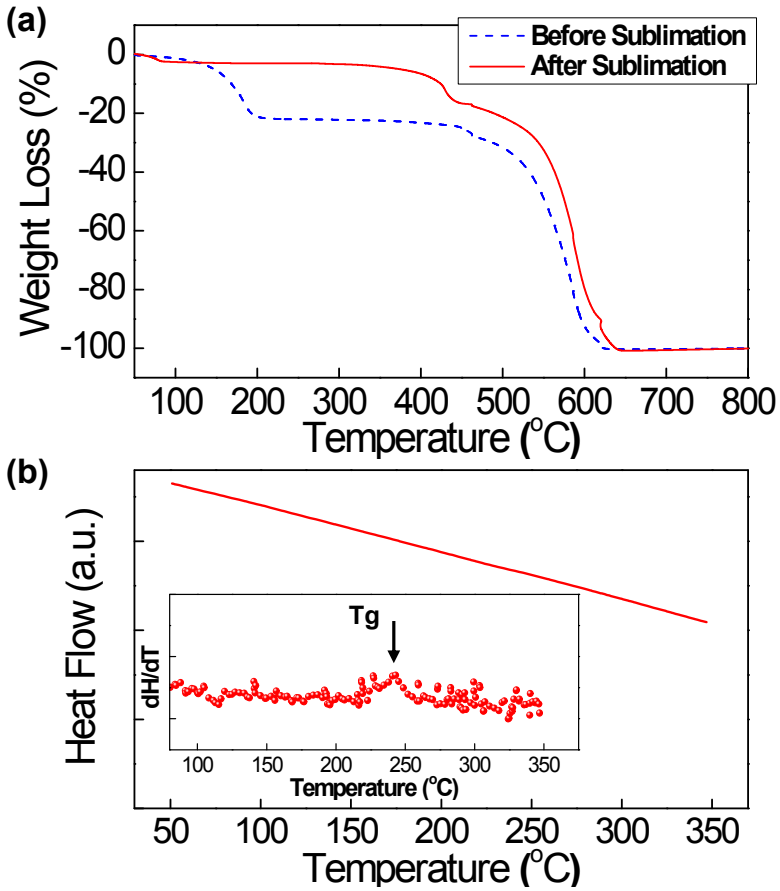

Fig. S1 (a) TGA thermogram of Bphen-PMDI powders before and after vacuum purification (sublimation). (b) DSC thermogram of Bphen-PMDI powders (This is a different measurement run from Fig. 2b in the main text): The inset shows the differential plot (dH/dT) to find the onset point of Tg because a clear inflection position could not be observed from the heat flow curve.

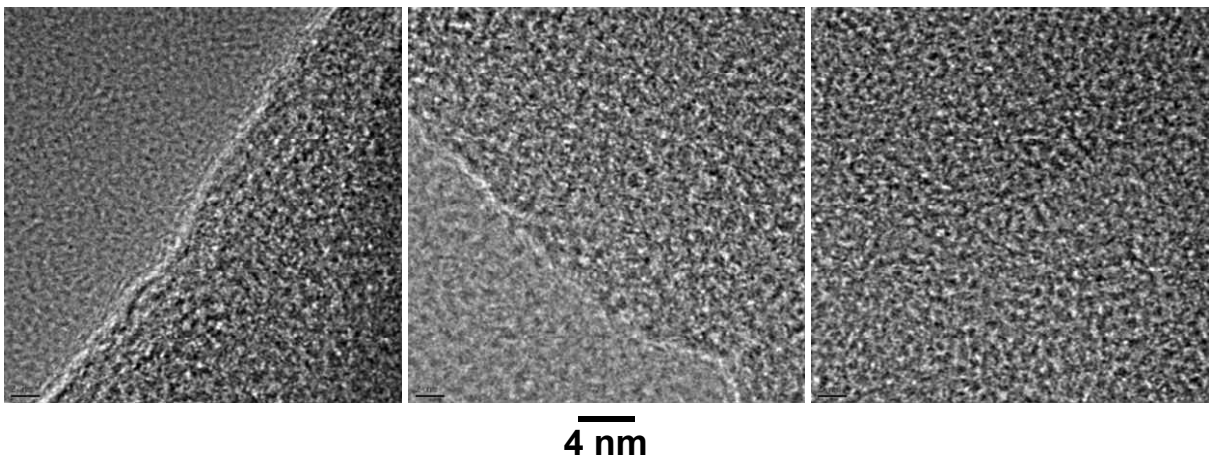

Fig. S2 HRTEM images of Bphen-PMDI powders: (a) full image of Fig. 2a, (b) different position at the boundary of the TEM grid, and (c) different position of only Bphen-PMDI on TEM grid.

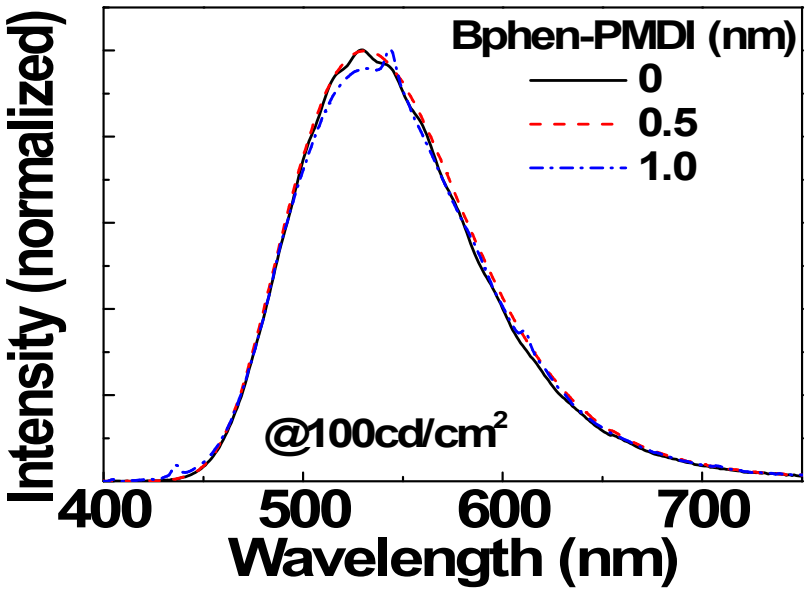

Fig. S3 EL spectra of OLEDs with the Bphen-PMDI layer, which were measured at the luminance of 100 cd/m^2.

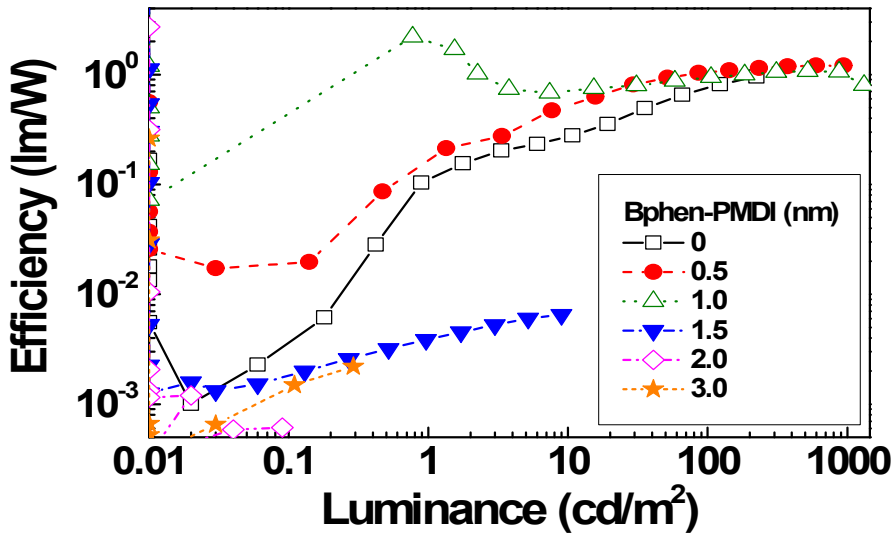

Fig. S4 Logarithmic plot of luminous efficiency and luminance for the OLEDs with the Bphen-PMDI layer.

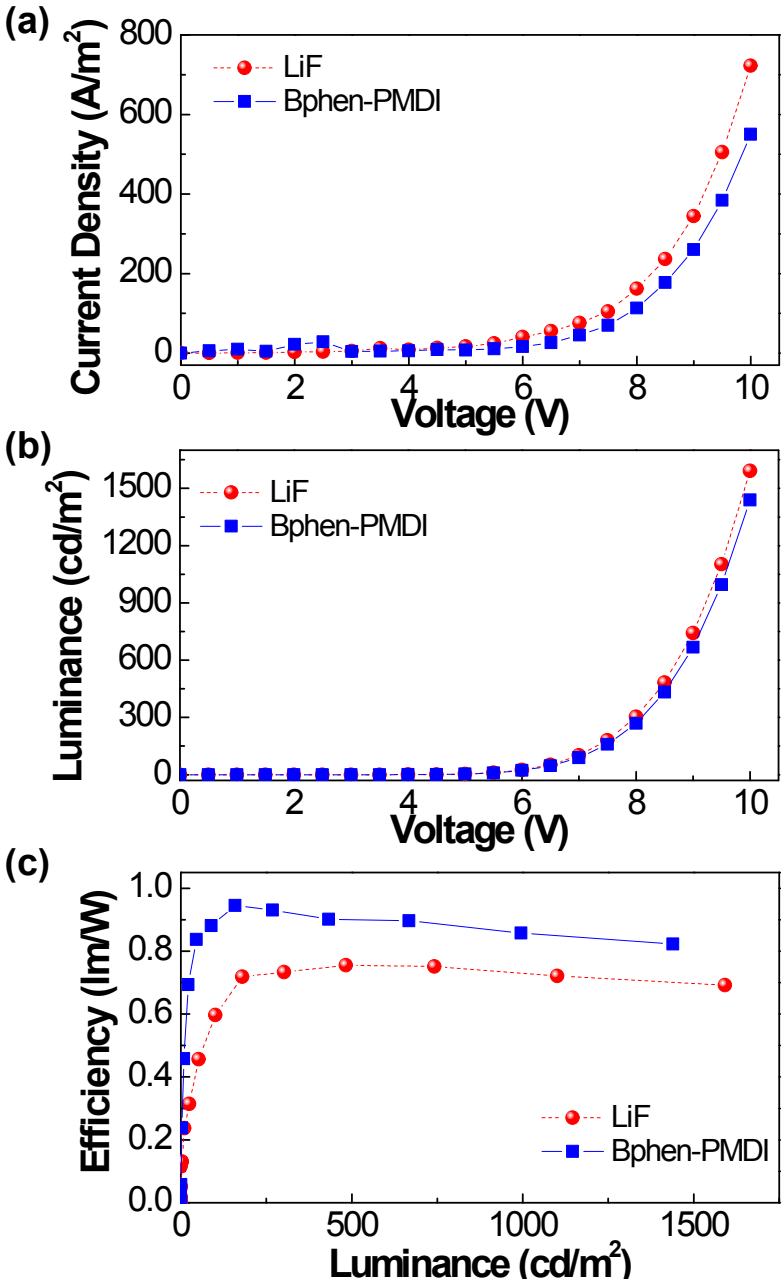

Fig. S5 Comparison of the device performances between the LiF layer (1 nm) and the Bphen-PMDI layer (1 nm): (a) J-V, (b) L-V, and (c) power efficiency.

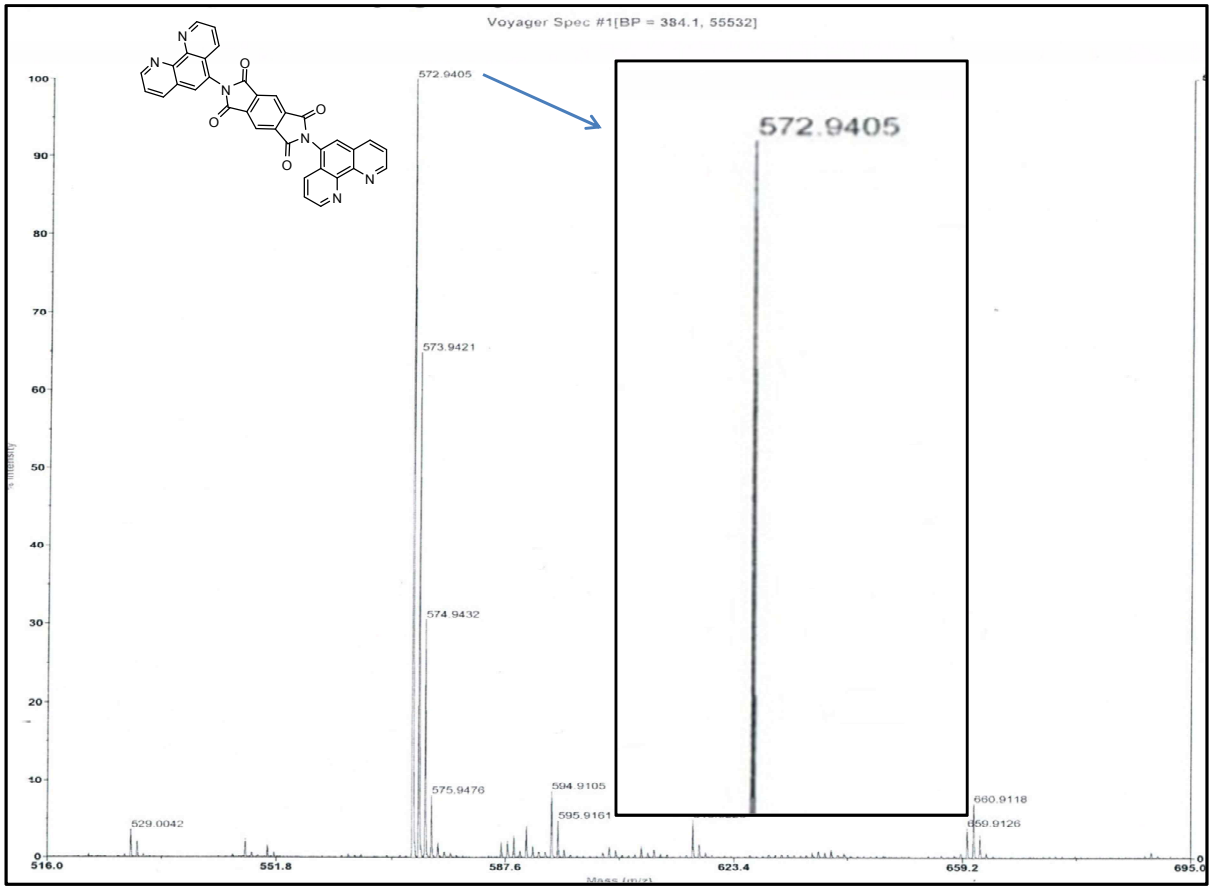

Fig. S6 MALDI-TOF-MS spectrum of the Bphen-PMDI powder (matrix: α-cyano-4-hydrocinnamic acid): The major peak was measured at m/z = 572, while other small peaks in the higher mass ranges can be attributed to the adducts between the ionized Bphen-PMDI and the degraded components from the Bphen-PMDI powder which are formed during the specimen preparation step using an acid solution (dichloromethane + 10% formic acid) because the present Bphen-PMDI powder is insoluble in common organic solvents (see Fig. S7 for example).

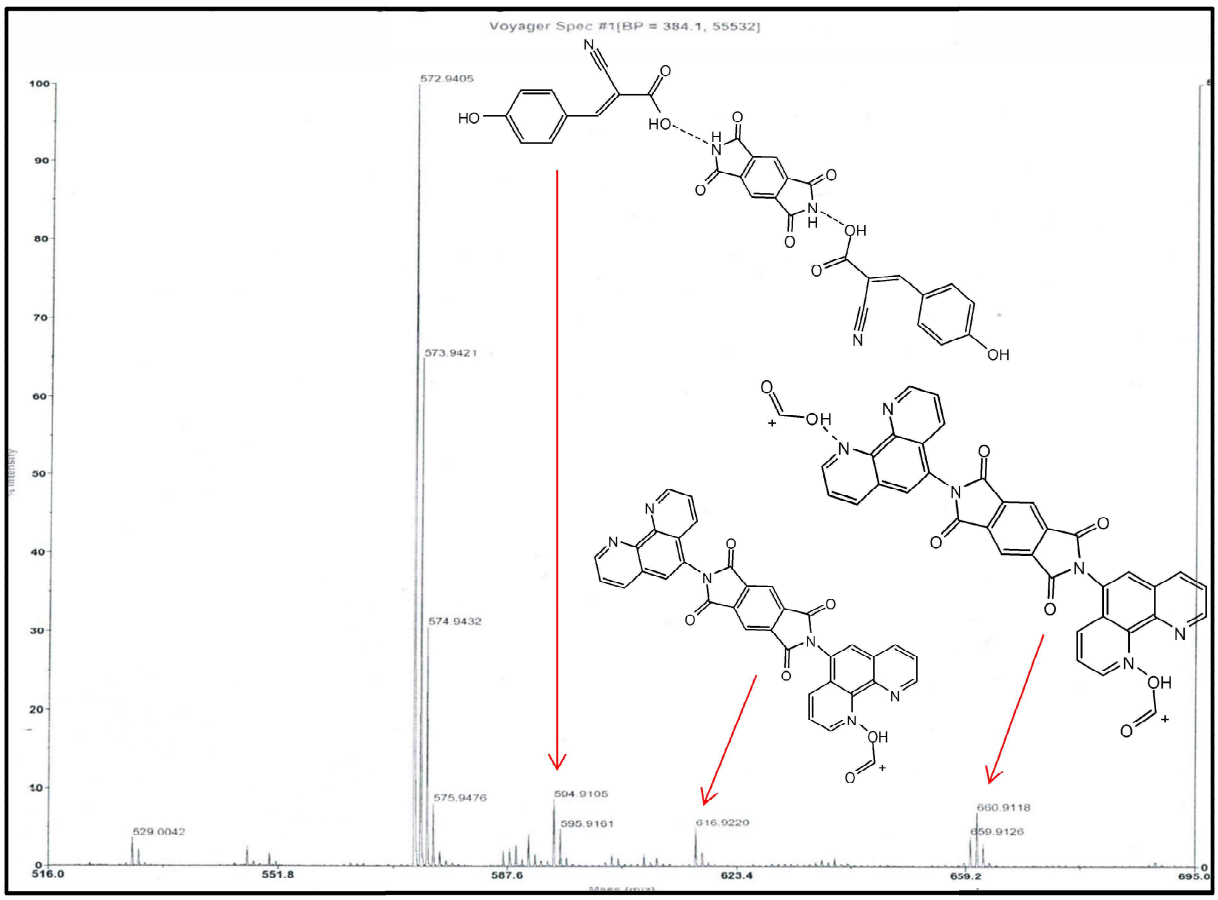

Fig. S7 Assignment of possible adducts between the ionized Bphen-PMDI and the degraded components from the Bphen-PMDI powder which are formed during the specimen preparation step using an acid solution (dichloromethane + 10% formic acid) for the MALDI-TOF-MS spectrum in Fig. S6.

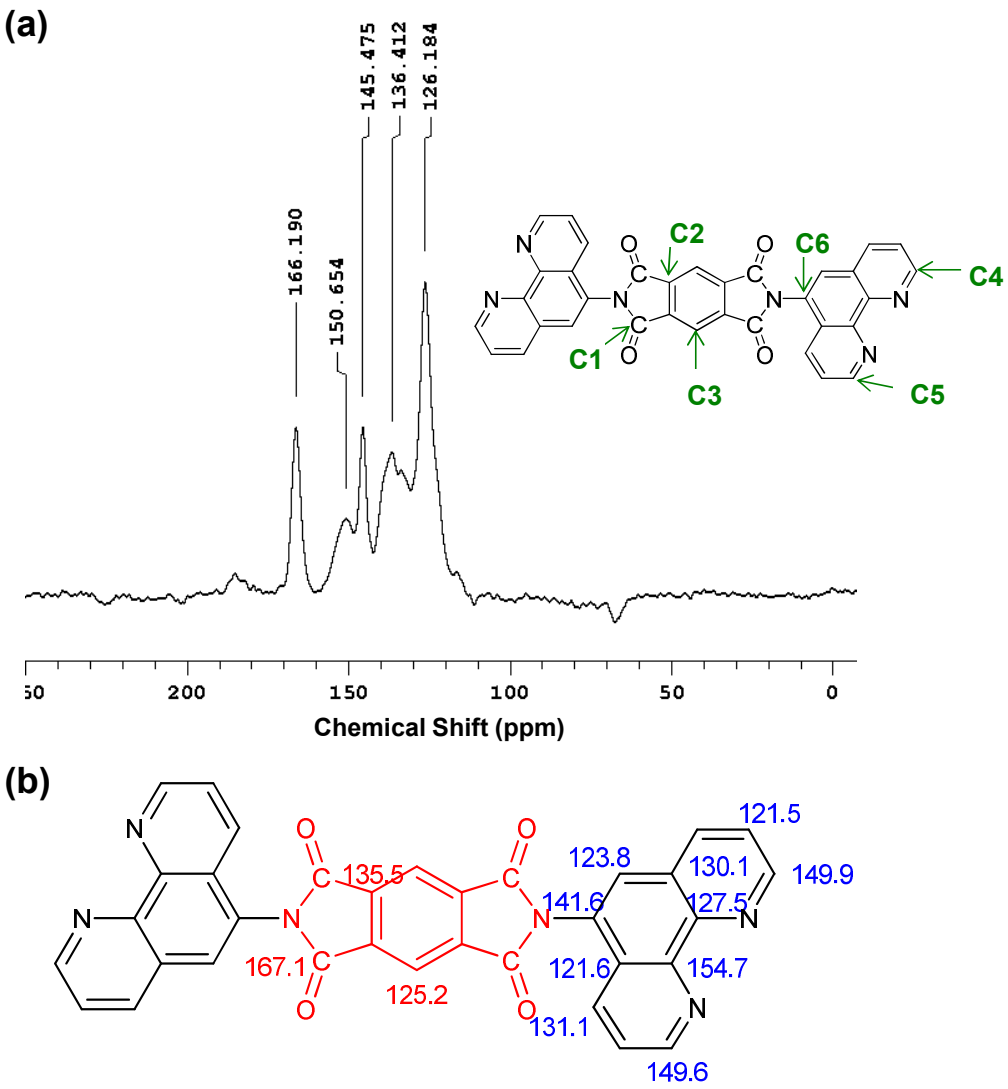

Fig. S8 (a) Solid-state ^{13}C-NMR spectrum of the Bphen-PMDI powder and (b) the simulation result of single Bphen-PMDI molecule (using ChemBioDraw Ultra - CambridgeSoft): (1) PMDI unit: C1 (measured = 166.19ppm, simulated = 167.1ppm); C2 (measured = 136.5ppm, simulated = 135.5ppm); C3 (measured = 126.184ppm, simulated = 125.2ppm); (2) Phenanthroline unit: C4/C5 (measured = 150.654ppm, simulated = 149.9ppm/149.6ppm), C6 (measured = 145.475ppm, simulated = 141.6ppm). We note that the Bphen-PMDI material is insoluble in common organic solvents so that conventional liquid-state NMR measurements were impossible. As usually observed in the solid-state NMR measurements, it should be noted that the peaks measured here are quite broad.

Fig. S9 Photograph for the solubility test of the Bphen-PMDI powder in solvents for NMR measurement: (a) DMSO-d_6, (b) Bphen-PMDI in DMSO-d_6, and (c) Bphen-PMDI in $CDCl_3$. The solid concentration of the Bphen-PMDI powder in the solvents was 30 mg/ml. As observed from the solutions (b) and (c), the Bphen-PMDI powder is not dissolved but roughly dispersed so that they could not be used for the liquid-state NMR measurement.